



HAL
open science

Lunar Surface Gravimeter as a lunar seismometer: Investigation of a new source of seismic information on the Moon

Taichi Kawamura, Naoki Kobayashi, Satoshi Tanaka, Philippe Lognonné

► **To cite this version:**

Taichi Kawamura, Naoki Kobayashi, Satoshi Tanaka, Philippe Lognonné. Lunar Surface Gravimeter as a lunar seismometer: Investigation of a new source of seismic information on the Moon. *Journal of Geophysical Research. Planets*, 2015, 120 (2), pp.343-358. 10.1002/2014JE004724 . insu-02559880

HAL Id: insu-02559880

<https://insu.hal.science/insu-02559880v1>

Submitted on 30 Apr 2020

HAL is a multi-disciplinary open access archive for the deposit and dissemination of scientific research documents, whether they are published or not. The documents may come from teaching and research institutions in France or abroad, or from public or private research centers.

L'archive ouverte pluridisciplinaire **HAL**, est destinée au dépôt et à la diffusion de documents scientifiques de niveau recherche, publiés ou non, émanant des établissements d'enseignement et de recherche français ou étrangers, des laboratoires publics ou privés.

RESEARCH ARTICLE

10.1002/2014JE004724

Key Points:

- Data from Apollo 17 LSG were reevaluated with a seismic point of view
- LSG data were used in source locations of moonquakes
- Located previously unlocatable deep moonquake nests with the additional data

Correspondence to:

T. Kawamura,
kawamura@ipgp.fr

Citation:

Kawamura, T., N. Kobayashi, S. Tanaka, and P. Lognonné (2015), Lunar Surface Gravimeter as a lunar seismometer: Investigation of a new source of seismic information on the Moon, *J. Geophys. Res. Planets*, 343–358, 120, doi:10.1002/2014JE004724.

Received 9 SEP 2014

Accepted 6 JAN 2015

Accepted article online 10 JAN 2015

Published online 26 FEB 2015

Lunar Surface Gravimeter as a lunar seismometer: Investigation of a new source of seismic information on the Moon

Taichi Kawamura¹, Naoki Kobayashi², Satoshi Tanaka², and Philippe Lognonné¹

¹Institut de Physique du Globe de Paris, University Paris Diderot - Sorbonne Paris Cité, Paris, France, ²Institute of Space and Astronautical Science, Japan Aerospace Exploration Agency, Kanagawa, Japan

Abstract Lunar seismology has always suffered from the limited number of seismic stations and limited coverage of the seismic network. Additional seismic data are necessary to probe the lunar interior in depth. Instead of a costly new deployment of seismometers, the aim of this study is to investigate the possibility of using the Apollo 17 Lunar Surface Gravimeter (LSG) as a lunar seismometer. The LSG was designed to detect gravitational waves (associated to change in the curvature of spacetime) and tidal ground motion on the Moon, but the data were not investigated for seismic use partially because of a malfunction of the instrument. We first evaluated the influence of the malfunction through comparison with other Apollo seismic data and found that the effect of the malfunction is small, and the LSG detected seismic signals in a manner that was consistent with those of the other Apollo seismometers. Then we carried out source location with the additional station of the LSG. We relocated previously located deep moonquake nests to evaluate the influence of the LSG data, which are generally noisier than other Apollo seismic data. Then we located deep moonquake nests that were previously unlocatable. Forty deep moonquake nests were examined, and we located five new nests. One newly located nest, A284, was most likely to be located on the farside. This series of analyses indicates that the LSG functioned as a lunar seismometer, and that its data are useful for improving seismic analyses with the previous seismic data set of the Moon.

1. Introduction

Since the successful Apollo Mission, geophysical data obtained on the lunar surface have been an essential source of information on the inner structure of the Moon. These investigations remain today unique, as the only post-Apollo missions able to provide new geophysical data of the Moon have been lunar orbiters.

One of the most successful investigations was achieved by seismic analyses of data from the Apollo Passive Seismic Experiment (PSE). Five seismic stations (Apollos 11, 12, 14, 15, and 16) were deployed during the Apollo missions [Lammlein *et al.*, 1974] (Figure. 1). While the station of Apollo 11 stopped observation after 21 days [Latham *et al.*, 1969], other stations observed lunar seismic events until the termination of Apollo observation in 1977. Five and one half years of network observations of four seismic stations were carried out on the Moon (Table 1) [Lammlein *et al.*, 1974; Nakamura *et al.*, 1982]. The network was deployed on the lunar surface and formed an almost equilateral triangle with stations 12 and 14 at one corner (Figure. 1). During these observations, more than 13,000 seismic events were recorded and cataloged [Nakamura *et al.*, 1981], with the latest count of 13,058 events (please refer to the last updated catalog at <ftp://utig.ig.utexas.edu/pub/PSE/catsrepts/>).

The seismic data obtained on the Moon have contributed to various investigations of the lunar interior (see reviews in Lognonné [2005] and Lognonné and Johnson [2007]). In the early 1980s, all the seismic data obtained by the PSE were compiled and used in investigations of the inner structure model of the Moon [e.g., Goins *et al.*, 1981; Nakamura, 1983]. Several layered structures were reported, and the crust/mantle boundary was reported to be at about 58 km depth. Other discontinuities and characteristic features (e.g., the low-velocity layer) explain the observed seismic features [e.g., Nakamura, 1983]. However, the sparse ray density in deep regions and uncertainties in arrival time readings leave uncertainties in these estimations, especially on the deep structure [e.g., Lognonné *et al.*, 2003; Nakamura, 1983, 2005]. In the 2000s, more powerful computers have enabled further analyses of the seismic data. Khan *et al.* [2000] reinterpreted the data using an inverse Monte Carlo sampling method and constructed a new model of the lunar interior.

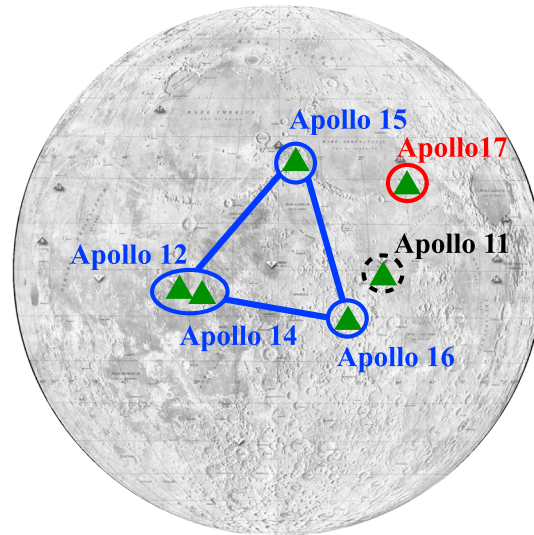


Figure 1. Location of Apollo stations on the Moon. Seismic observation was carried out at stations 11, 12, 14, 15, and 16. Observation of the seismometer at the Apollo 11 site lasted only ~3 weeks, and it did not contribute to the network observation. No seismometer was deployed at the Apollo 17 site; however, the gravimeter, a good candidate as a source of additional seismic information, was deployed at the site.

The Moon has a partial melt boundary at 480 ± 15 km radius, a core mantle boundary at 330 ± 20 km radius, and an inner core boundary at 240 ± 10 km radius. Garcia et al. [2011] used seismic and geodetic data to estimate the deep inner structure of the Moon. They gave 380 ± 40 km for the core radius and implied the existence of a liquid outer core beneath the core mantle boundary. They also estimated the core density to be 5200 ± 1000 kg/m³.

There is no doubt that the Apollo seismic data have been an important source of information in the investigation of the lunar interior. At the same time, however, limitations of the Apollo data have prevented us from uncovering its detailed features.

The limited number of seismic stations and the limited observable area of the seismic network on the Moon are two of the major problems in lunar seismology. The seismic network that was limited to four seismic stations with a maximum base line of 1100 km could not provide global coverage of the Moon. One issue that results from these limitations is difficulty in detecting farside events (i.e., events whose source longitude is $>90^\circ\text{E}$ or $>90^\circ\text{W}$). Since all the stations are located on the nearside (longitude $<90^\circ\text{E}$ or $<90^\circ\text{W}$), fewer farside events than nearside events have been identified thus far. However, analysis of farside events is critical for understanding the deep inner structure of the Moon. The deepest useful direct P or S rays from previous studies sounded the lunar interior down to between 1100 km and 1300 km depth at most [e.g., Lognonné et al., 2003; Nakamura, 1983; Goins et al., 1981]. Given that the radius of the Moon is 1738 km, the central 400 km of the Moon is probed only through the weak reflected phases reported by Weber et al. [2011] and

Independent studies of Lognonné et al. [2003] and Gagnepain-Beyneix et al. [2006] used inversion of travel time and receiver function analysis [Vinnik et al., 2001] to reinvestigate the seismic data. Estimations of both Khan et al. [2000] and Lognonné et al. [2003] indicated thinner crusts than early models constructed during the Apollo era. The estimates ranged from 45 ± 5 km, 38 ± 3 km, 34 ± 6 km, and 30 ± 2.5 km, respectively, for Khan et al. [2000], Khan and Mosegaard [2002], Chen et al. [2006], and Lognonné et al. [2003]. The estimations here are the values for the Procellarum KREEP (potassium, rare earth element, and phosphorus) Terrane region of the Moon which was sampled with the present seismic network on the lunar nearside. Wieczorek et al. [2013] used these seismic constraints to anchor the high-resolution data from GRAIL (Gravity Recovery and Interior Laboratory) mission proposing different crustal models anchored either by the Lognonné et al. [2003] 30 km thickness or the 38 km thickness of Khan and Mosegaard [2002]. Using established methods of terrestrial seismology, Weber et al. [2011] reported core phases in the lunar seismograms. They concluded that the

Table 1. Apollo Seismic Stations and Observation Periods

	Installation	Termination	Position
Apollo 11	7/21/69	8/27/69	0.4°N, 23.28°E
Apollo 12	11/19/69	9/30/77	3.04°S, 23.42°W
Apollo 14	2/5/71	9/30/77	3.65°S, 17.48°W
Apollo 15	7/31/71	9/30/77	26.08°N, 3.66°E
Apollo 16	4/21/72	9/30/77	8.97°S, 15.51°E
Apollo 17	12/12/72 ^a	9/30/77	20.11°N, 30.46°E

^aFor Apollo 17, installation of the LSG is indicated in the table.

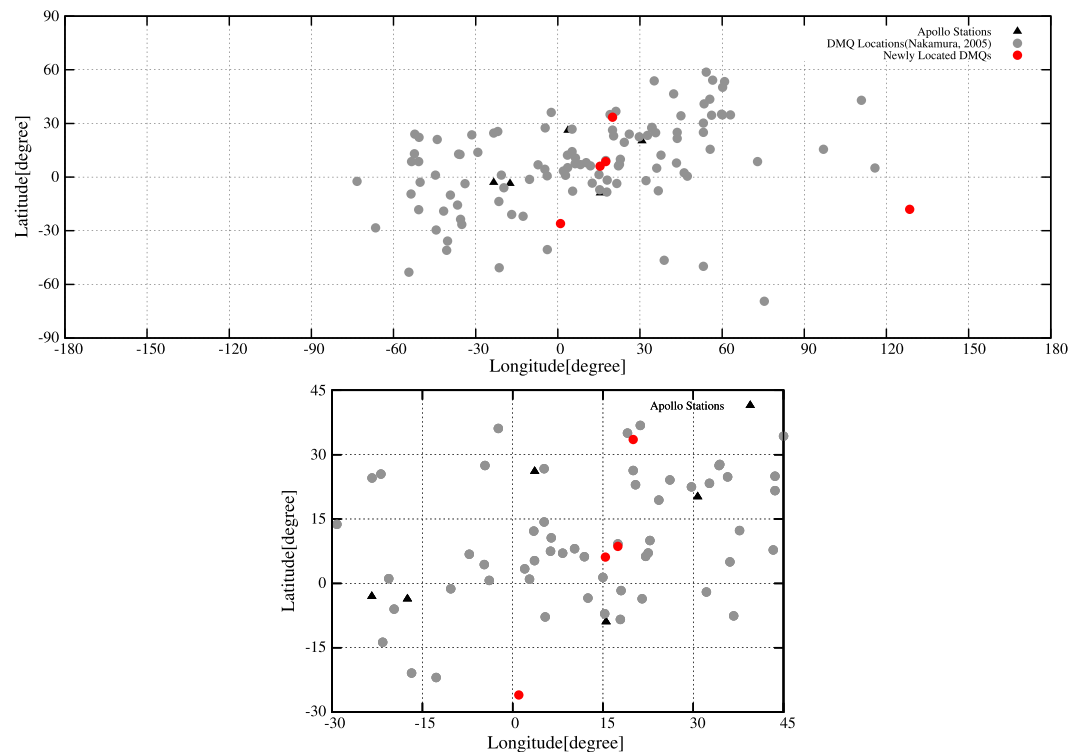


Figure 2. Spatial distribution of known deep moonquake nests and newly located nests. Black triangles denote the locations of the Apollo stations. Gray circles denote the known nests listed in Nakamura [2005]. Red circles indicate the new deep moonquake nests located in this study. (top) A global distribution and (bottom) the distribution around the seismic network.

Garcia et al. [2011], which can, however, be resolved only through the stack of all available Apollo records and not individually on seismic records, as future lunar instrumentation could do [*Yamada et al.*, 2013]. This leaves large uncertainties in our understanding of the deep inner structure of the Moon.

Second, lack of detection of farside events also makes it difficult to determine global seismicity on the Moon. Figure 2 depicts the distribution of deep moonquake nests located in a previous study. These deep moonquake nests concentrate on the nearside and distribute in the southwest to northeast region of the lunar nearside [*Lammlein et al.*, 1974]. Distribution of seismic sources and seismicity can be an implication of the inner tectonic features of the Moon. Thus, whether such a distribution represents the real seismicity of the Moon or a mere bias of the observation network is an important issue to be investigated.

Finally, while we have little information on seismicity on the lunar farside, a number of events in the current data set remain unlocated and/or unclassified, and may be on the lunar farside. One fourth of the seismic events detected during the observation are unlocated and/or unclassified [e.g., *Nakamura*, 2003]. For example, *Nakamura* [2005], who reclassified the deep moonquake events into nests with the waveform correlation method, concluded that 60 of the 166 deep moonquake nests that had been identified could not be located due to a lack of available arrival picks in the data set. This corresponds to 3000 of 7200 individual deep moonquake events.

To overcome such problems, additional seismic data and further observation are essential, and several future projects have been proposed [*Shiraishi et al.*, 2010; *Mimoun et al.*, 2012]. However, since the termination of Apollo seismic observation on 30 September 1977, there has been no seismic observation on the Moon. This study proposes to use other scientific instruments as new sources of seismic information for further seismic analyses on the Moon. While Apollos 11 through 16 had a seismic observation package as a payload (PSE package), Apollo 17 did not have such seismic observation package and was not regarded as a seismic station. Although it did have geophones for the Lunar Seismic Profiling Experiment, it did not run long-term observation, and the data are difficult to use in seismic analyses with other Apollo PSE data [*Kovach and Watkins*, 1973].

However, Apollo 17 had a gravimeter as its payload, which also performs as a vertical accelerometer. This Lunar Surface Gravimeter (LSG) can be regarded as a seismometer and can be used in seismic analyses with seismic data from other seismic stations. Although such a possibility was well accepted [e.g., *Giganti et al.*, 1977], no close investigation of the data have been conducted from a seismological perspective.

Figure 1 depicts the Apollo seismic network and the Apollo 17 station, where the LSG is deployed. Apollo 17 is also on the lunar nearside; thus, the network is still limited to the lunar nearside. At the same time, since the LSG is at station 17 outside the traditional observation network and occupies the east end of the new network (Figure 1), the observable area is likely to expand eastward. This may raise the possibility of finding new seismic sources that were out of range with the previous network, especially in the Eastern Hemisphere.

In addition to the expanded coverage, such a “new” station will provide additional constraints for source location. Most of the unlocated events lack a sufficient number of signal arrival times to locate the events [*Nakamura*, 2005]. An additional station may provide additional arrival picks and enable us to locate events that were previously unlocatable. Source locations of such unlocated seismic events will be informative in the analysis of source distribution and seismicity of the Moon.

To investigate the possibility of using LSG data as seismic data, we first review the general status of the instrument. We then compare the data with the other seismic observations of Apollo. After we confirmed that the LSG was detecting seismic signals in a consistent manner with other Apollo seismometers, we discuss the application of the LSG data to the seismic analyses. We evaluate the possible bias or error that can contaminate our results. Finally, we use both Apollo seismometer data and LSG data to locate seismic sources. We conduct source locations in two conditions. The first is seismic events that were already located with the previous data set. These results were compared with those of previous studies, and we discuss the contribution and/or bias of the LSG data to the source location. The second is unlocated seismic events. One of the most important contributions of the additional data is their potential to enable source location of previously unlocatable sources. Thus, this will be our aim in evaluating the usability of the LSG as an additional seismometer. With these first results, we discuss the usability of the LSG data and its contribution to further seismic analyses.

2. Lunar Surface Gravimeter

2.1. General Status

The Lunar Surface Gravimeter (LSG) was part of the Apollo lunar surface experiment package (ALSEP) of Apollo 17 [*Giganti et al.*, 1973]. The primary objective of the LSG was to search for gravitational waves predicted by Einstein’s general theory of relativity, and the second objective was to measure the tidal deformation of the Moon [*Giganti et al.*, 1973].

In the LSG, a LaCoste-Romberg type of spring-mass suspension was used to sense changes in the vertical component of local gravity [*Giganti et al.*, 1973]; for general information on a LaCoste-Romberg type of gravimeter, please refer to reviews such as *Aki and Richards* [2002] or *Havskov and Alguacil* [2004], and references therein. The instrument was a sensitive balance with masses, springs, and lever systems with electronics for observing acceleration in the frequency range of 0 to 16 Hz [*Giganti et al.*, 1973]. The data were sampled with ~ 0.02 s time step, which corresponds with the Apollo short-period seismometer. Specification for the data acquisition of the instrument is summarized in Table 2.

To adapt to both Earth testing and lunar operation, the sensor mass is modified with the addition or removal of small weights [*Giganti et al.*, 1973]. The mass-adding mechanism is also used for caging the sensor beam during transfer to the lunar surface. The sensor beam is caged by clamping the upper mass and the pan.

2.2. Malfunction and Reconfiguration

Apollo 17 was launched on 7 December 1972, and the LSG was deployed on the lunar surface on 12 December 1972 [*Bates et al.*, 1979]. When the LSG was deployed on the Moon, the sensor beam could not be balanced in the proper equilibrium position even with all the available mass added to the sensor beam assembly [*Giganti et al.*, 1977]. The only time the beam moved was when the caging mechanism was in physical contact with it. It was then determined that an error in arithmetic made by the vendors had not been corrected while developing the instrument [*Giganti et al.*, 1977]. Thus, though the instrument was capable of

Table 2. Data Specification of Apollo 17 Lunar Surface Gravimeter

		Comments
Sampling rate (sample per seconds)	48	29 samples per 0.60377 ms
Dynamic range(bits)	10	0–1023
Output voltage (V)	±10	
LSB	0.0195	0.098 nm/bit
Frequency range (Hz)	0–16	Seismic Mode
Sensitivity: Seismic mode high gain (V/nm)	0.199	
Sensitivity: Seismic mode low gain (V/nm)	0.000376	
Observation period ^a	1972/12/12–1977/9/30	Data Archived: 1976/3/1–1977/9/30

^aDates are formatted as year/month/day.

detecting small variation in terrestrial gravity, it was just barely outside the tolerance for variation of lunar gravity. The mass needed to null the sensor beam was larger than the maximum mass that could be added using the mass-adding mechanism; thus, the sensor beam was left at the upper stop [Giganti et al., 1977].

Several reconfigurations of the instrument were implemented by the Apollo 17 crew members in an effort to determine whether the LSG was functioning. To center the sensor beam with the limited mass available with the mass-adding mechanism, the sensor beam was pulled down using the caging mechanism by physically contacting the beam. This operation was successful. By adding a downward force of 0.17×10^{-2} N, the beam was balanced and could be operated as a vertical accelerometer and seismometer [Larson and Weber, 1974]. The LSG detected a seismic signal near the terminator crossing [Giganti et al., 1977]. This seismic signal observed using the LSG is most likely a thermal moonquake caused by a sudden change in temperature [Duennebier and Sutton, 1974]. This was strong evidence that the LSG was functioning as a lunar seismometer. Observation indicated background noise higher than those implied by the Passive Seismic Experiment and the Lunar Seismic Profiling Experiment [Lauderdale and Eichelman, 1974]. After a series of reconfigurations and observations, it was concluded that the LSG was detecting signals from local seismic events.

However, these reconfigurations changed the instrument sensitivity. In general, the instrument ended up in a narrower-frequency band than the designed sensitivity. It appears that the LSG is less sensitive than the designed sensitivity at 1 Hz and lower but has comparable sensitivity at frequencies exceeding 1 Hz. We can see the resonant frequency at ~1 Hz. During the reconfiguration, the resonant frequency was tuned to

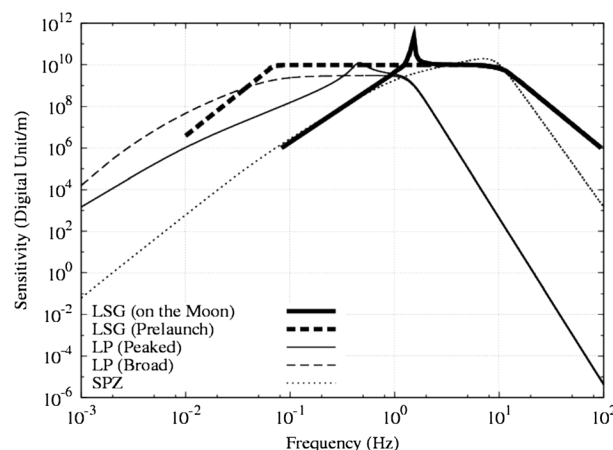


Figure 3. Sensitivity of the LSG compared with that of other Apollo seismometers. Lines indicate the LSG (solid line for sensitivity on the Moon and dashed line for designed sensitivity), Apollo long-period seismometer (thin line for peaked mode and thin dashed line for broad mode), and Apollo short-period (dotted) seismometer. The transfer functions are taken from Lammlein et al. [1974] for the Apollo seismometers and from Giganti et al. [1977] for the LSG.

match the frequency range that is suitable for lunar seismic observation [Larson and Weber, 1974]. Figure 3 indicates the sensitivities of the LSG and Apollo seismometers. The sensitivity of the LSG is comparable or even higher than those of other Apollo seismometers at frequencies above 1 Hz. Comparison of the sensitivity of Apollo seismometers and the LSG implies that the malfunction and the reconfiguration did change the sensitivity of the instrument but that it is still sufficient for lunar seismic observation.

After 5 years of observation, it was concluded that the LSG could not detect evidence of lunar free-mode oscillation or meaningful data for gravitational radiation. Giganti et al. [1977] did note that “a large number of lunar seismic events were observed and these data have been useful for the seismology investigations.” However, there is little indication that the LSG data were used in

seismological investigations, and the data were left unanalyzed for more than 40 years, and never used in any paper dealing with the location of moonquakes or inversion of interior structure.

2.3. LSG Data

After the malfunction, subsequent reconfiguration and change in the sensitivity, the LSG could not achieve its primary objective. Though observation using the LSG was carried out from LSG deployment on 12 December 1972 until 30 September 1977, *Lauderdale and Eichelman* [1974] concluded “no provision has been made to supply data from this experiment to the National Space Science Data Center.” Thus, most of the LSG data have not been released, and a large portion of the data are still not available. The scientific data of Apollo were generally processed and compiled at NASA’s Johnson Space Center and delivered to the principal investigators of each scientific instrument until 19 February 1976 [e.g., *Bates et al.*, 1979]. The data were then submitted to the National Space Science Data Center (NSSDC) and archived. These data are preserved and provided to researchers for scientific use. LSG data were not submitted for the reason above and are not available at NSSDC. Thus, the data from 12 December 1972 to 19 February 1976 are not currently accessible.

By mid-1975, analysis contracts with most of the individual principal investigators were terminated [*Bates et al.*, 1979]. However, observation of the ALSEP was still being conducted. The data flow from the five stations on the lunar surface continued, and the cost of the data processing remained constant. To decrease the cost, data processing was transferred to the University of Texas at Galveston. The transfer was completed in March 1976, and the data were sent to the University of Texas until 30 September 1977, which was the termination of the Apollo observation [*Bates et al.*, 1979]. The data archived at the University of Texas were undecoded; it contained all the ALSEP telemetry data, including the LSG data. This data are called “ALSEP 24 h Work Tape Files” and are available at NSSDC (NSSDC ID: PSPG-00738). This undecoded data were not extracted as scientific instrument data and were not converted into physical values. While seismic data were already archived [*Nakamura*, 1992], the data must be extracted and interpreted for each scientific objective for other instruments. The ALSEP data format for the Work Tape is given in *Nakamura* [1992], and the assignment of each bit of the ALSEP data to parameters of various instruments can be obtained from other documents [e.g., *Lauderdale and Eichelman*, 1974]. Referring to such documents, we were able to extract the LSG data from the Work Tape data.

The currently available LSG data are thus limited to those from 1 March 1976 to 30 September 1977, included in the Work Tapes, except for the period of high-bit-rate observation. This corresponds to 20% of the entire data. Although data coverage is rather low, close investigation of the data has great implications for verifying the function of the LSG as a seismometer and the application of its data to further seismic analyses. Thus, the data are meaningful and worthwhile for more detailed analyses.

3. Detection of Seismic Signals With the LSG

3.1. Event Detection With the LSG

Though previous researchers were aware that the LSG was detecting seismic signals, there are little reports that discuss its events detection in detail [e.g., *Giganti et al.*, 1977]. In this study, we reconfirm that the LSG was reacting to seismic signals and evaluate its long-term efficiency for event detection. To verify that the LSG was reacting to lunar seismic events, we examined LSG data during seismic events that were identified with Apollo seismometers at other stations. For these events, we referred to the lunar seismic event catalog of *Nakamura et al.* [1981]. As pointed out in the previous chapter, the LSG had a higher noise level than the other Apollo seismometers. To better identify seismic signals within the noisy data, we examined the data in both time and frequency domains. Figure 4 presents an example of a seismogram and a spectrogram of the LSG data during a seismic event. *Nakamura et al.* [1981] reported that a deep moonquake event from A07 nest reached the seismic network near 12:50. The signal is noisy in the time domain, so it is difficult to identify. However, we can identify a clear signal in the frequency domain. The spectrogram indicates that the energy of the seismic signals is concentrated within a narrow-frequency band of 1 to 2 Hz. The filtered signal in the time domain is also shown in the figure. Filtering significantly improves the signal-to-noise ratio. Here we filtered the data with a frequency band from 1.4 Hz to 1.8 Hz, which corresponds to the resonant frequency of the instrument.

Previous studies classified three typical types of lunar seismic event: deep moonquakes, shallow moonquakes, and meteorite impacts [e.g., *Lammlein et al.*, 1974; *Nakamura et al.*, 1982]. We examined signals from these three types of events to confirm that the LSG was reacting to them. To deal with the high noise level of the LSG

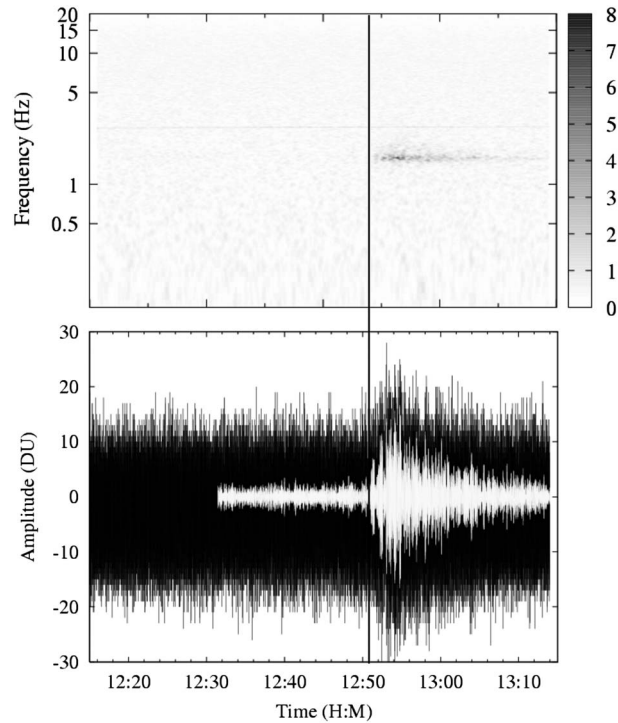


Figure 4. Spectrogram and waveform of a deep moonquake on 11 April 1976, observed using the LSG. The cataloged arrival time is 12:51, denoted by the black line. (top) The spectrogram and the (bottom) the seismogram. The spectrogram with the x axis of time and y axis of frequency illustrates the time variation of the spectrum. The color contour represents the spectral intensity in Digital Unit, which is 10 bits integer output from analog to digital converter. The raw seismogram is presented in black, and the filtered seismogram is presented in white in Figure 4 (bottom). We recognize that the LSG definitely caught the lunar seismic events reported in *Nakamura et al.* [1981]. The signal is seen in both time and frequency domains. The signal-to-noise ratio of the raw seismograms may not always be sufficient to identify seismic signals. The figures also indicate that band-pass filtering effectively reduces noise. The cataloged time is from *Nakamura et al.* [1981].

data, the data were examined in both time and frequency domains, as was done in the previous analyses. In all cases, the LSG was reacting to seismic signals and detecting seismic events. The spectrograms indicate that the narrow-frequency band is common to the three types of event. In addition to the spectral peak at 1 to 2 Hz, we observed another peak at 10 Hz for shallow moonquakes. The peak we see uniquely on shallow moonquakes is most likely due to a spectral feature specific to shallow moonquakes [*Nakamura et al.*, 1974]. *Nakamura et al.* [1974] found that the spectral power of meteoroid impact drops quickly over 1 Hz, whereas that of shallow moonquakes has a constant value up to 5 Hz and drops gradually. Although the reason for the sharp peak is unclear, this high-frequency energy, which was detected uniquely with shallow moonquakes using other seismometers, was also observed with the LSG. These results suggest that the LSG functioned as a vertical seismometer and was capable of detecting various types of lunar seismic events. The features of the seismic signals observed using the LSG also seem to be consistent with those detected by the other Apollo seismometers. The results also indicate that though the background noise is high, the signal-to-noise ratio of the LSG data can be significantly improved with proper noise reduction.

Next, we evaluate the long-term event detection of the LSG. According to *Nakamura et al.* [1981], the number of

seismic events recorded in the Work Tape files is as presented in Table 3. In this study, we selected some typical seismic events and some interesting targets (listed below). All shallow moonquakes and meteorite impacts extracted from the binary data were examined. Deep moonquake events were selected according to the deep moonquake nests to which they were classified. We selected events from the nest that met our objectives. First, we chose three deep moonquake nests that were close to station 17: A06, A07, and A22. Second, we chose nest A01, which is one of the most active and well-investigated deep moonquake nests identified thus far. Since the nests are either close to the station and/or active, seismic signals from these

Table 3. Number of Seismic Events During the Work Tape Observation Period [*Nakamura et al.*, 1981]

Type of Events	Number of Events (1972 Through 1977)	Events During Work Tape Observation (3/1/76 Through 9/30/77)
Artificial impact	9	0
Meteorite impact	1743	203
Shallow moonquakes	28	3
Deep moonquakes	7245	970
Unclassified	3533	453
Total	12558	1629

Table 4. Deep Moonquake Nests Used in This Study^a

	Nests
Well-determined deep moonquakes	A01, A06, A07, A22
Farside deep moonquakes	A29, A33, A218, A244, A245
Unlocated deep moonquakes	A02, A23, A31, A43, A69, A72, A75, A79, A80, A89, A90, A94, A98, A104, A205, A206, A207, A208, A210, A211, A213, A214, A215, A219, A220, A222, A225, A227, A232, A235, A253, A254, A256, A263, A264, A265, A270, A274, A284, A289

^aClassification of deep moonquake nests is from *Nakamura* [2003, 2005]. Nests that are missing from the list of unlocated deep moonquake nests in *Nakamura* [2005] are ones whose event is not recorded in the available LSG data.

nests are expected to have higher signal-to-noise ratios than other deep moonquake nests and to be detected most efficiently using the LSG. Third, we examined deep moonquake events from the nests located on the lunar farside by *Nakamura* [2005]. Finally, we examined the deep moonquake events from nests that were reported to be unlocatable by *Nakamura* [2005]. These nests were examined to test the potential of the LSG to expand the observable area of the seismic network and to reexamine the unlocated and/or unclassified seismic events. Table 4 lists the deep moonquake nests investigated in this study. We also examined some unclassified events that were detected by two or more stations of the original network in order to investigate the possibility of locating and classifying previously unlocated and unclassified events.

The results are summarized in Table 5. We counted the seismic events that indicated a sign of seismic signal, regardless of its quality. Therefore, the results here should be regarded as preliminary results of the first seismic investigation of the LSG data. To use the data in further analyses (e.g., arrival time readings or source locations), the data may need to be reevaluated and the number of usable events may decrease. Thus far, 844 events have been examined, 191 of which were detected by the LSG. The number of events detected by the LSG is 20% of the examined events. With the higher noise level of the LSG, detection of seismic signals was more difficult than with other Apollo seismometers, and the number of detected events is smaller. Small events that are far from station 17 were undetectable using the LSG. Notably, the number of detected events for the A01 deep moonquake nest is small (6 out of 46) because of the large distance between station 17 and nest A01. In contrast, almost all the events from nest A22 were detected (12 out of 13). Table 6 summarizes the deep moonquake detection of the LSG for four clusters. Though detectability depends on both epicentral distance and magnitude, there is a clear dependence on distance. This tendency is also the same for farside events. While events from close and/or active nests were detectable using the LSG, events from a distant nest (e.g., A218) were out of the range.

In this study, we examined only known seismic events. However, there may also be seismic events detected using only the LSG. On 26 March 1976 3:00, we can identify large seismic signal, which were not reported in *Nakamura et al.* [1981]. These were not detected with other Apollo seismic stations and possibly a local impact close to station 17. Such events may be found throughout the observation period. This might be informative for studying seismicity or impact rates on the Moon. However, since such events are detected at only one station, the information that can be extracted from these events might be limited. We will not discuss these events further in this paper; however, this subject should be investigated in the future.

4. Data Analysis

4.1. Arrival Time Readings

We confirmed that the LSG functioned as a lunar seismometer, and events detected by the other Apollo seismometers were also detected by the LSG. Our next step is to use the LSG data in seismic analyses with other

Table 5. Number of Seismic Events Examined Thus Far and Number of Events Detected by the LSG

	Examined	Detected by the LSG
Deep moonquake	485	134
Meteoroid impact	191	28
Shallow moonquake	3	3
Unclassified	165	26
Total	844	191

seismic data. We performed arrival time readings and seismic source locations using both the LSG and other Apollo seismic data. For the LSG data, we first confirmed that the signal-to-noise ratio was sufficient to read arrival times. Due to the noise of the instrument, the initial rising of the arrival phase is, however, hidden

Table 6. Number of Deep Moonquake Events That Were Detected by the LSG Well-Located Deep Moonquake Nests

Source Region	Distance From A17 (deg)	Number of Events Examined	Number of Events Detected by the LSG
A01	75.2	46	6
A06	31.2	21	8
A07	21.3	19	12
A22	12.1	13	12
Farside Deep Moonquake Nests			
Source Region ^a	Distance From A17 (deg)	Number of Events Examined	Number of Events Detected by the LSG
A29	40.5	6	3
A33	83.6	5	4
A218	104.0	17	3
A244	26.6	2	1
A245	42.4	4	1
Unlocated Deep Moonquake Nests			
Source Region	Number of Events Examined	Number of Event Detected by the LSG	
A23	9	1	
A75 ^b	8	3	
A79 ^b	5	2	
A104	3	1	
A211	2	1	
A214	1	1	
A227 ^b	1	1	
A232	2	2	
A263	2	2	
A274	1	1	
A284	4	3	
A289	7	1	
A319 ^b	2	1	
A320	1	1	
A366	2	2	
A394	2	1	
A401	1	1	
A407	1	1	
A412	3	1	
A435 ^b	1	1	

^aIn Nakamura [2005], A282 was also classified as a farside deep moonquake but was excluded from the table since there was no event recorded in the Work Tape.

^bNot all events during the Work Tape observation were examined because of the unexpected data gap in the LSG data.

by noise, and the reading might generate systematic bias, which must be evaluated. It should also be noted that for deep moonquakes, these processes were run for each nest, not for individual events. Deep moonquake events occur periodically at specific nests, and the waveforms of the same set of a deep moonquake nest and a station are almost identical. Thus, to improve the signal-to-noise ratio, waveform correlation and waveform stacking were performed. This method has commonly been used for deep moonquake analyses [e.g., Nakamura, 2003, 2005; Lognonné et al., 2003].

Arrival time readings are one of the most basic processes in seismic analyses. However, there are no established methods for arrival time reading for lunar seismic data, and the results differ among studies. Generally, for lunar seismic events, intense scattering and poor signal-to-noise ratios make it difficult to read arrival times accurately. Nakamura [2005] compared the arrival times of deep moonquakes from five studies and found that arrival times can differ by tens of seconds and as much as 100 s. This implies that

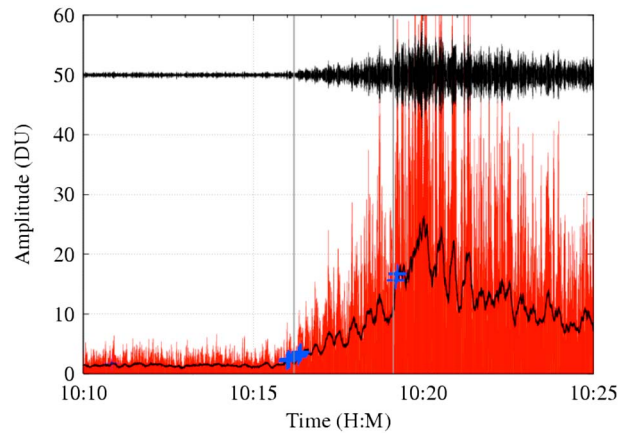


Figure 5. Example of arrival time reading. The figure explains the processed signals we used in our arrival time readings. The red signal is the absolute value of the examined waveform. The raw signal of the waveform is shown at the top in black. The black line shows an amplitude profile calculated with a 10 s time window and the blue pluses are the data points with signal amplitude significantly larger than the background signal level and regarded as candidates for the arrival times. Two gray lines show P and S arrival read from the candidates.

arrival time readings are strongly influenced by subjective identification of the individual investigator and, in the specific lunar case, that errors classically too large for Earth seismic analysis can still be acceptable for lunar studies, due to the paucity of data (an obvious example is when a deep moonquake has been detected on only a few of the Apollo data and is unlocated). On the other hand, automatic arrival time reading is easy and more robust to subjective bias of human eyes. While event triggering mechanism or automatic arrival time detection is carried out in terrestrial seismology, this was not applied to lunar seismic data mainly because of the low signal-to-noise ratio and strong scattering that obscure the signal arrivals. Noisy data can result in a systematic bias in the arrival times. There is a clear tradeoff between the two approaches, and they should be carefully chosen.

In this study, we will take a quasi-automatic approach. This will enable us to exclude the subjective judgments as much as possible. In addition, since the main aim of this study is to test the usability of the LSG data as seismic data, the requirement for the precision of arrival times and source location is not very severe. We regard the arrival readings to be good enough if they do not distort our source locations significantly. In other words, if our source location matches results from the previous studies within the range of our error bars, we regard we were able to read arrival times with sufficient precision. It is true that this approach leaves some systematic bias to source locations. Thus, we discuss such bias through comparison between our source locations and previous locations for one of the best-located sources.

For quasi-automatic detection of arrivals, we regarded a signal arrival as a significant change in amplitude. To detect such significant change, we take the following steps. First, we took the amplitude profile by taking the moving average of the absolute value of amplitude. Let a time series of seismic signal be a_i , and we can express

the amplitude profile as $p_i = \frac{1}{n+1} \sum_{j=i-n/2}^{i+n/2} |a_j|$. The time window used in the moving average constrains the reading

error of arrival times, and this was tuned by changing n in the equation. We take a longer-time window with m data points of the amplitude profile and calculate the average value and standard deviation (σ) of the m ($>n$)

data. This can be expressed as $\bar{p}_i = \frac{1}{m} \sum_{j=i-m+1}^i p_j$ for the average and $\sigma_i^2 = \frac{1}{m} \sum_{j=i-m+1}^i (p_j - \bar{p}_i)^2$ for the standard

deviation. This average value is regarded as a representative background signal level and is compared with the following data point to define the change in amplitude. This change in amplitude is regarded as the signal amplitude, which is defined as $s_{i+1} = p_{i+1} - \bar{p}_i$. This signal amplitude is then compared with the standard deviation calculated earlier. When the signal amplitude exceeds 3σ of the m data, in other words, when $s_{i+1} > 3\sigma_i$, we consider the change in amplitude as significant and regard it as a candidate for signal arrival. We continuously move the window of m data points with time to examine whether the signal at each data point is significantly larger than the background noise level. This method is similar to the long-term average (LTA) and short-term average (STA) triggering system used in terrestrial seismology, where the former time window refers to the STA and the latter time window defined to estimate the background signal level refers to LTA. Arrival time reading error is defined using the time window we adopt to calculate the average amplitude. These processes are described in Figure 5. Since lunar seismic signals are noisy and suffer from intense scattering, this method does not always give unique solution for phase arrivals. In Figure 5, we see two groups of arrival candidates, each

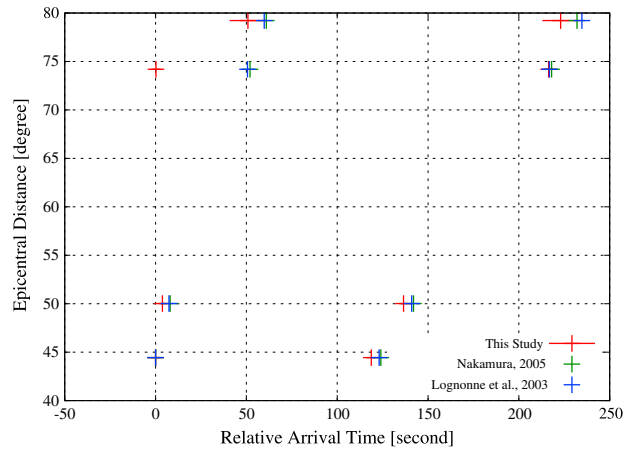


Figure 6. Comparison of arrival time reading from three studies. The figure represents arrival times for the A07 deep moonquake. Since all studies use waveform stacking to improve the signal-to-noise ratio, the arrival times are compared in relative values, which is the difference from the first detected signal. Since our study use the quasi-automatic arrival time reading that is subject to be influenced by the S/N ratio, our arrival times tend to be earlier than those of other studies.

arrival time readings of P phases at far station. As it was pointed out before, the aim of this study is to test the usability of the LSG data in seismic analyses with other Apollo seismic data, mainly in seismic source locations. Thus, even if the individual arrival times differ, we regard the difference as insignificant if the resulting source locations are not scattered significantly. This will be discussed more in detail in the following section. In addition to this, we will evaluate the systematic bias that will be imposed from our quasi-automatic arrival time readings in the following section.

corresponding to P and S arrival. In such cases, unless the method was detecting clear glitch or unexpected nonseismic signals, either we take the earliest one as the arrival (either P or S depending on the phase we are searching) or take both detection into account and include this as a reading error in the arrival time.

This method was first confirmed with other Apollo seismometers. Our arrival time readings are compared with those of other studies in Figure 6. We see that our arrival time reading is earlier than other studies.

This can be regarded as a systematic error within our method. Since we use background noise to define our criteria, the method is affected by the signal-to-noise ratio of the data. We can recognize this as a larger deviation of

4.2. Seismic Source Location of Known Seismic Stations and Evaluation of Systematic Bias in the Analyses

After reading arrival times using the seismograms, we locate the seismic sources. First, we locate seismic sources that are well located in previous studies. The aim of this first attempt is to evaluate the usability of the LSG data in the source location with other Apollo seismic data. In addition to this, we evaluate the possible bias and error that can contaminate our analyses. In this study, we focus on deep moonquakes as targets. Deep moonquakes are the most common seismic event on the Moon and are an important source of information for lunar seismology. Thus, evaluation of LSG data in the context of its contribution to deep moonquake source location can be used as a benchmark of the seismic use of LSG data. Note that deep

Table 7. Results of the Source Location From Various Studies

		Latitude (deg)	Longitude (deg)	Depth (km)
A06	with LSG	43.9 ± 2.8	59.3 ± 4.3	806 ± 68
	without LSG	43.5 ± 2.9	57.0 ± 4.1	833 ± 81
	Nakamura [2005]	43.5 ± 2.9	55.5 ± 9.5	844 ± 33
	Lognonné et al. [2003]	49.7 ± 1.0	54.7 ± 0.7	860 ± 11
A07	with LSG	25.4 ± 1.5	57.9 ± 3.7	940 ± 42
	without LSG	25.1 ± 1.5	55.5 ± 3.6	951 ± 70
	Nakamura [2005]	25 ± 1.7	53.2 ± 8.0	893 ± 27
	Lognonné et al. [2003]	24 ± 0.8	53.7 ± 0.7	900 ± 12
A22	with LSG	27.8 ± 3.6	50.2 ± 4.9	616 ± 74
	without LSG	26.9 ± 5.2	41.5 ± 7.7	784 ± 241
	Nakamura [2005]	21.6 ± 1.8	43.6 ± 5.9	788 ± 29
	Lognonné et al. [2003]	—	—	—

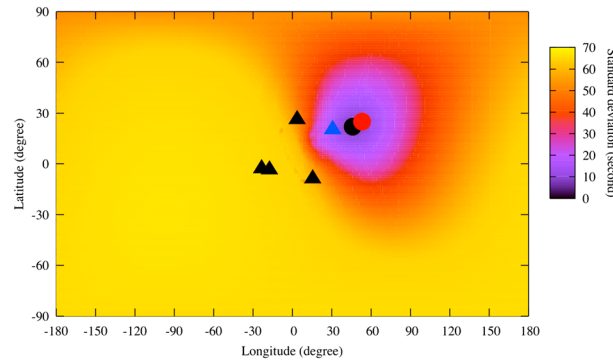


Figure 7. Example of source location of deep moonquake nests. The figure shows nest location of A07 deep moonquake nest estimated with four seismic stations of Apollo and the LSG. The color contour shows the residual estimated from the grid search. By seeing the global residual map, we can ensure that our inversion did not drop into some local minimum. The red circle is the location estimated in this study, and the black circle is the location from Nakamura [2005]. The black triangles refer to the Apollo stations, and the blue triangle is the LSG station.

moonquake events from the same nest were stacked before reading arrival times, and the seismic source is located for each nest. This also enables us to improve the signal-to-noise ratio of the LSG data.

We located the deep moonquake nests by a linearized inversion of arrival times using the lunar velocity model of Nakamura [1983]. Since the aim of this study was to evaluate the usability of the LSG data as seismic data and to perform the first seismic analysis using the LSG, we focused only on locating the source regions; the velocity model was fixed, and we did not investigate differences between velocity models. First, we performed an inversion to obtain four parameters: latitude, longitude, depth, and event time. If the inversion did not converge, in order to limit the number of

potential parameters, we fixed the depth to 933 or 750 km, the typical values of the source regions previously determined by Nakamura *et al.* [1982], and recalculated the source locations. To ensure that the inversion did not drop into some local minimum far from the true location, we tried to optimize the initial values for the inversion. We ran a coarse grid search of latitude, longitude by 1°, and depth by 10 km and searched for temporary hypocenter, which will be used as an initial value for the inversion.

We use A06 and A07 deep moonquake nests to evaluate our source locations. These nests are located in both Nakamura [2005] and Lognonné *et al.* [2003] with P and S arrival from all four Apollo stations and can be regarded as a well-located deep moonquake nests. In addition, they are close to the LSG and large number of events from these nests was detected by the LSG. Our results are summarized in Table 7. Figure 7 depicts the results for A07. Figure 7 also depicts the global residual map from the grid search we used to define our initial value. We carried out source location in several settings. First, we carried out source locations with arrival times only from Apollo seismometers without LSG data. These results can be directly compared with source locations from previous studies. This will enable us to evaluate the bias that derives from

quasi-automatic arrival time readings. If we compare our results with results from two previous studies [Nakamura, 2005; Lognonné *et al.*, 2003], our results are closer to those from Nakamura [2005]. Presumably, such tendency was a consequence of using the velocity model from Nakamura [1983] as it was done in Nakamura [2005]. The difference between the two previous studies can be regarded as the deviation of source location that derives from using the different velocity models. When we compare our results with those of Nakamura [2005], our results overlap with the previous study within the range of our error bar. Thus, we can claim that our arrival time reading is good enough to retrieve the results from the previous study. Our location errors are large especially when we compare them with those of Lognonné *et al.* [2003]. This is

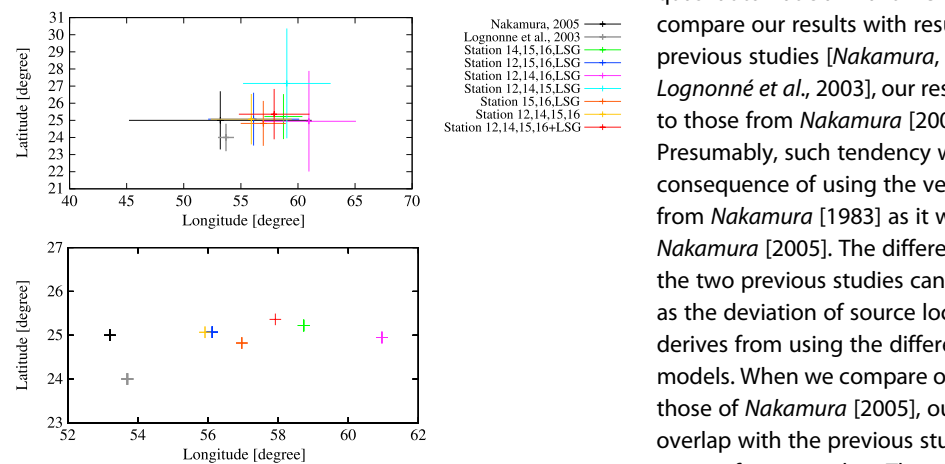


Figure 8. Deviation of source location with different sets of arrival picks. (top) The source location with their location errors. We can see that our results are consistent within the range of the error, including one result from Nakamura [2005]. (bottom) The close up of Figure 8 (top). The deviation is mostly on the longitude direction, and this is due to the geometric configuration of the network.

mainly due to larger arrival reading error we expect from our method. The deviation in obtained source locations is one of a tradeoffs of applying the quasi-automatic arrival time reading method. The lower signal-to-noise ratio is likely to delay the signal detection. This will result in the farther locations for the studied sources, which can be observed in Figure 8. The direction that the source location will be shifted depends on the difference in signal-to-noise ratio for each station. This can also be regarded as the geometric configuration of the station network and the studied nest. The shifts we have on our results are few degrees, which are comparable to our location error, and this is smaller than the possible deviation that is derived from the adapted velocity model. This error is sufficient to test the usability of the LSG data in source locations with other Apollo seismic data. The quasi-automatic arrival time reading is likely to have some bias, which presumably dependent on signal-to-noise ratio, and this shifts the source location from the real position. However, the shift is comparable to the location error we expect from our arrival time readings. Thus, we should note that there is a bias in our source location, but the bias is included in the location error and the true location should be in the range of the error we expect from the arrival times.

Compared to other Apollo seismometer, the LSG has lower signal-to-noise ratio. Thus, the bias on the arrival time readings that derive from our methods may be larger for the LSG. This needs to be evaluated to test the usability of the LSG. The location estimated with five seismic stations including the LSG is also summarized in Table 7, and the result for A07 is also presented in Figures 7 and 8. When we compare our result with four stations without the LSG and with five stations with the LSG, we can evaluate the bias that result from the additional but noisier data. Ideally, the two results should be identical, which is not the case since we have error on our arrival time readings and on the model as well. For this aim, we should compare the results from our own source location with four and five stations so that we can minimize the influence of the deviation of arrival times. Here we used our results for A06, A07, and A22. First, we compared our results from four stations to five stations (Table 7). When we add the LSG data to the source locations, the estimated source shifts toward the farther location. As it was discussed earlier, the noisier data may result in delayed arrival times and it is reasonable to have farther source location with the additional data. The shift should be mainly attributed to the added arrival times of the LSG, while the contribution of the other stations shall not be neglected since we have nonzero residuals for the inversion from four stations as well. To evaluate how much the arrival of the LSG can be shifted by low signal-to-noise ratio, we randomly shifted our arrival times to the LSG arrival times and studied how the source location will be shifted by the reading error. Given that the low signal-to-noise ratio tends to delay the arrival pick, we randomly shifted our LSG arrival reading from -40 to 10 s to account for the possible reading error. When we take the example of the A07 deep moonquake nest, the source location estimated with five stations can be shifted so that the location matches the location estimated with four stations by adding artificial reading error to the arrival times of the LSG. For the best match, the P and S arrivals of the LSG need to be shifted by ~ 10 s and ~ -6 s, respectively. Negative time shift refer to delayed arrival times for our arrival picks, in other words, our arrival times need to be shifted earlier to match the reference source location. Our expectation of the reading error was about 10 s, which is comparable with the deviation we got. On the other hand, while our S arrival shows some delay as expected from the lower signal-to-noise ratio, our P arrival was earlier than the arrival expected from the source location estimated with four stations. This may be an indication that our identification of arrival times is more erroneous compared to our expectations. The same analyses for other nests also indicate that applying the time shifts to the arrival times enable us to shift the source location toward the locations estimated with four stations. The time shift needed to match the two inversions about ~ 10 s for A06 and ~ 20 s for A22. This can be regarded as a potential reading error on the LSG arrival times. The time shift is larger for A22. The larger shift is most likely due to the smaller number of arrival picks used in the inversions. As it was the case for Nakamura [2005], P arrivals on some stations were not clear and were not used in the inversion (stations 12 and 15 for Nakamura [2003] and stations 12 and 14 for our arrival picks). At the same time, since we have nonzero residuals for our inversions with four stations and the estimated locations differ from those of other studies, it is highly possible that the locations we estimated with four stations, which we used as reference values, are off from the true value. Thus, the time shifts estimated previously should be regarded as upper limits. When we refer to the previous study [i.e., Lognonné *et al.*, 2003], they accepted 10 s as a maximum reading errors used in their inversion. Our potential reading error is larger than this by a factor of 2. This partially due to the quasi-automatic arrival time reading we adopted, and this may be improved by further investigation. To test the consistency and robustness of our source location, we ran source locations with decimated number of station and arrival times. Even if we replace other Apollo

Table 8. Estimated Sources of Unlocated Deep Moonquakes

	Latitude (deg)	Longitude (deg)	Depth (km)
A211	-26 ± 5	1 ± 2	933 ^a
A227	23.5 ± 5.3	20.0 ± 3.4	933 ^a
A263	8.6 ± 1.6	17.5 ± 3.2	750 ^a
A284	-18.4 ± 11.9	128.5 ± 15.5	0–1738 ^b
A289	6.1 ± 1.5	15.4 ± 2.4	933 ^a

^aFixed value.

^bThe nest can be at any depth in the Moon due to the poor signal-to-noise (S/N) ratio of the data. We confirmed that the longitude and the latitude of the nest do not change significantly when we fixed the depth to realistic values for deep moonquakes.

stations with the LSG, the source location is identical within the range of our error bar. This is evidence that the LSG data were detecting seismic signals in a consistent manner with other Apollo seismometers, and the data can be used in source locations of seismic events.

We evaluated possible bias that may result from the noisier additional station. We will now use the LSG data in source location of unlocated

seismic sources. It is true that the LSG has higher noise level compared to the other Apollo seismometers, and arrival times provided from the data can be more erroneous compared to the other data. On the other hand, seismic sources that were considered to be unlocated did not have a sufficient number of arrival picks, an additional arrival times from the LSG data will be nonetheless meaningful to further investigate the unlocated seismic sources. Here we focus on the deep moonquake nests, which were considered unlocatable by *Nakamura* [2005]. According to *Nakamura* [2005], 60 source regions did not provide sufficient arrival time readings to locate the source and are yet to be located. Forty of the 60 deep moonquake nests had seismic events during the observation period of the Work Tape files and are used in this study. As discussed earlier, locating previously unlocated seismic sources is important in terms of investigating the global seismicity of the Moon, and it is meaningful to reanalyze such events with additional seismic data of the LSG. The previous test with known deep moonquake nests implies that the arrival time we read with the LSG data has some additional reading error or bias on the arrival times due to the smaller signal-to-noise ratio. Thus, we assume that our arrival times for unlocated deep moonquake nests also have some potential reading errors, and we carried out the same statistical approach as we did in the previous tests. We added random reading error to the LSG arrival times and studied how the source locations shift with the potential reading error. The arrival time will be shifted within -40 to 10 s. Given that the time shifts for the close deep moonquake nests are ~ 10 s, we take 40 s for the max potential error. The scatter we obtain from the test would be regarded as possible errors in the source locations, in addition to those we obtain analytically from reading errors and inversion process.

5. Discussion

All the events from the 40 unlocated deep moonquake nests were examined to test whether the data are useful for arrival time readings and source locations. As it was done in the other studies and our previous investigations, the data from the same deep moonquake nest were stacked to improve the signal-to-noise ratio, if possible. After the stacking, five deep moonquake nests out of 40 had signal-to-noise ratios sufficient to read arrival times and source location. The results are summarized in Table 8 and Figure 2. *Nakamura* [2005]

pointed out the possibility that these nests were on the farside; however, our calculation suggests that four of the five nests are on the nearside and that only A284 is located on the farside. The depth error of the nest A284 is expected to be large because of the large reading errors of the arrival times, as well as the geometric configuration of the station and the seismic source. To confirm that the location of A284 does not change drastically according to its depth, we also carried out source locations by fixing their depth to typical source depths for deep moonquakes (750, 933, and 1000 km). The results were within the

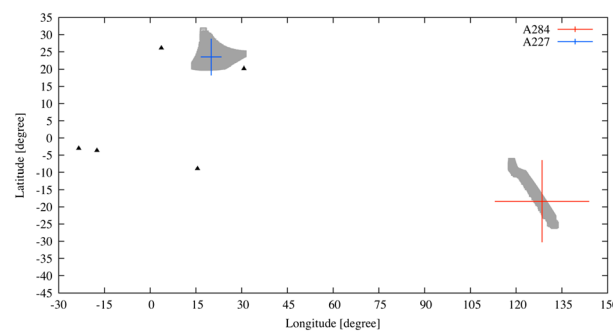


Figure 9. Shift of seismic source location deriving from additional reading error on the LSG arrivals. The black triangles refer to Apollo stations, and the gray marks are the scatter of the source locations.

range of the nominal location uncertainty. Thus, our analyses strongly suggest that A284 is most likely located on the farside of the Moon, and that it is one of the deep moonquake nests that are farthest from the center of the seismic network. To consider potential reading errors that we might have overlooked in our estimations of location errors, we now discuss how the source locations shift with artificial reading error added to the arrival times of the LSG. Figure 9 shows the examples of the location shift we expect from additional reading errors. The results imply that the source location can change by about 10° with 40 s of arrival time reading error. Forty seconds of reading error is an arbitrary threshold we defined to test the scatter of source locations that derive from reading error. If we assume that we were able to identify the first signal that exceeded the noise level, the potential reading error depends on the noise level and rise times (time difference between the signal arrival and the maximum amplitude) of seismograms. The noise level of the LSG is independent of events or epicentral distance. The rise time is strongly affected by intense scattering of the Moon and may differ between events. *Blanchette-Guertin et al.* [2012] claims that the scattering feature of deep moonquakes do not differ significantly with epicentral distance. Thus, ideally the potential error within the identified arrival times should not differ significantly with events. Forty seconds of reading error is an arbitrary threshold but can be regarded as a conservative assumption of reading error for deep moonquakes, though it is still possible that we are misidentifying signal arrivals. When we compare our results from the unlocated deep moonquakes, the scatter of the source locations to the additional reading error was $\sim 10^\circ$ and about 20° for the worst case. Even if we consider the deviation, we can conclude that all the studied unlocated deep moonquake nests except for A284 are on the lunar nearside and the A284 nest is the only one that is likely to be on the lunar farside. Another notable point of A284 is that it is one of the most active currently located farside deep moonquake nests. Fifty-three events were observed for A284 during the entire observation period; such large number of events is comparable to the previously identified farside nest A33 (57 events), which is the most active and the best-located farside deep moonquake nest to date. The number of farside deep moonquake events increased by 40% with the newly located deep moonquake nest. Most deep moonquake nests had 50 or fewer events during the observation period, and both A33 and A284 can be regarded as relatively active deep moonquake nests. In terms of global lunar seismicity, it is interesting that a relatively active deep moonquake nest was located on the farside of the Moon.

6. Conclusions and Future Work

We reanalyzed the data of the LSG on Apollo 17 and evaluated these lunar seismic data. We confirmed that the LSG functioned as a lunar seismometer and detected signals from the major types of moonquakes: deep moonquakes, shallow moonquakes, and meteorite impacts. Given that the LSG had lower signal-to-noise ratio compared to other Apollo seismometers, we evaluated the possible bias that may contaminate our arrival time readings with the LSG data through source locations of known deep moonquake nests. Then, we performed source location for unlocated deep moonquakes pointed out in *Nakamura* [2005] and determined five new deep moonquake nests from 40 candidates. Among the newly located sources, nest A284 is on the lunar farside and was expected to be one of the farthest deep moonquakes found thus far.

We confirmed the usability of LSG lunar seismic data and demonstrated its usefulness in seismic analyses with other Apollo seismic data. Our next goal is to organize the LSG data from a seismic perspective and to extract information of the lunar interior structure using both LSG and PSE data. The data we studied is accessible in nondecoded form from NSSDC and in decoded form from Data ARchives and Transmission System (DARTS) project at Japan Aerospace Exploration Agency (JAXA) (<http://www.darts.isas.jaxa.jp/index.html.en>). The currently available data include only 20% of the entire observation period. The improvement expected from the limited data coverage is moderate, and larger data coverage will surely improve seismic analyses using the LSG data. Recovering data from other observation periods will be important for fully using the LSG data in seismic analyses. However, retrieving the lost LSG data will be challenging. The data were not archived in NSSDC, and the data given to individual investigators during the mission are possibly lost. Though the possibility might be low, the effort to archive the lost data should be continued. Further analyses of known seismic events and unlocated and/or unclassified seismic events with additional LSG data may enable more in-depth probing of the lunar interior. The additional station can contribute to characterize both local and global internal structure of the Moon. As *Chenet et al.* [2006] estimated local crustal thickness with impact events, the same estimation shall be possible at the station 17 site using the LSG data. On the other hand, if we are able to locate seismic events far from the Apollo stations, we could find raypaths that probe deeper into the Moon compared to the previous data set without the LSG. This will enable us to probe the structure of the

Moon deeper than before. Thus, attempt to locate unlocated and unclassified events using the additional data set should be continued and improved for further contribution of the LSG.

Acknowledgments

We would like to acknowledge Yoshio Nakamura at the University of Texas for his notable help. The information he gave us on the Apollo data and the documents he provided us were essential to understand the gravimeter data and interpret the results we obtained. T. Kawamura position is funded by CNES, who supported also this activity in the frame of the scientific preparation of SEIS/InSight. Additional support from the Campus Spatial Paris Diderot is also acknowledged. This work was also supported by JSPS KAKENHI grant 21–7206. All the data used in this study are now available at Data ARchives and Transmission System (DARTS) project at JAXA (<http://www.darts.isas.jaxa.jp/index.html>). This is IGP contribution 3594.

References

- Aki, K., and P. G. Richards (2002), *Quantitative Seismology*, 2nd ed., Univ. Science Books, Sausalito, Calif.
- Bates, J. R., W. W. Lauderdale, and H. Kernaghan (1979), ALSEP Termination Report, NASA Reference Publication RP-1036, p. 162.
- Blanchette-Guertin, J. F., C. L. Johnson, and J. F. Lawrence (2012), Investigation of scattering in lunar seismic coda, *J. Geophys. Res.*, *117*, E06003, doi:10.1029/2011JE004042.
- Chenet, H., P. Lognonné, M. Wieczorek, and H. Mizutani (2006), Lateral variations of lunar crustal thickness from the Apollo seismic data set, *Earth Planet. Sci. Lett.*, *243*, 1–14.
- Duennbier, F., and G. H. Sutton (1974), Thermal moonquakes, *J. Geophys. Res.*, *79*, 4351–4363, doi:10.1029/JB079i029p04351.
- Gagnepain-Beyneix, J., P. Lognonné, H. Chenet, and T. Spohn (2006), Seismic models of the Moon and their constraints on the mantle temperature and mineralogy, *Phys. Earth Planet. Inter.*, *159*, 140–166, doi:10.1016/j.pepi.2006.05.009.
- Garcia, R. F., J. Gagnepain-Beyneix, S. Chevrot, and P. Lognonné (2011), Very preliminary reference Moon model, *Phys. Earth Planet. Inter.*, *188*(1–2), 96–113.
- Giganti, J. J., J. V. Larson, J. P. Richard, and J. Weber (1973), Lunar Surface Gravimeter Experiment in Apollo 17 Preliminary Science Report, NASA SP-330, Washington, D. C.
- Giganti, J. J., J. V. Larson, J. P. Richard, R. L. Tobias, and J. Weber (1977), Lunar Surface Gravimeter Experiment Final Report, Univ. of Maryland Department of Physics and Astronomy, College Park, Md.
- Goins, N. R., A. M. Danity, and M. N. Toksöz (1981), Lunar seismology: The internal structure of the Moon, *J. Geophys. Res.*, *86*, 5061–5074, doi:10.1029/JB086iB06p05061.
- Havskov, J., and G. Alguacil (2004), *Instrumentation in Earthquake Seismology, Modern Approaches in Geophysics*, vol. 22, Springer, Dordrecht, Netherlands.
- Khan, A., and K. Mosegaard (2002), An inquiry into the lunar interior: A nonlinear inversion of the Apollo lunar seismic data, *J. Geophys. Res.*, *107*(E6), 5036, doi:10.1029/2001JE001658.
- Khan, A., K. Mosegaard, and K. L. Rasmussen (2000), A new seismic velocity model for the Moon from Monte Carlo inversion on the Apollo lunar seismic data, *Geophys. Res. Lett.*, *27*, 1591–1594, doi:10.1029/1999GL008452.
- Kovach, R. L., and J. S. Watkins (1973), Lunar Seismic Profile Experiment in Apollo 17 Preliminary Science Report, NASA SP-330, Washington, D. C.
- Lammlein, D., G. V. Latham, J. Dorman, Y. Nakamura, and M. Ewing (1974), Lunar seismicity, structure and tectonics, *Rev. Geophys. Space Phys.*, *12*, 1–2.
- Larson, J., and J. Weber (1974), Report on the Lunar Surface Gravimeter. [Available at <http://www.lpi.usra.edu/lunar/ALSEP/pdf/LunarSurfaceGravimeter.pdf>.]
- Latham, G. V., M. Ewing, F. Press, G. Sutton, J. Dorman, N. Toksöz, R. Wiggins, Y. Nakamura, J. Derr, and F. Duennbier (1969), *Passive Seismic Experiment in Apollo 11 Preliminary Science Report*, NASA SP-214, Washington, D. C.
- Lauderdale, W. W., and W. F. Eichelman (1974), *Apollo Scientific Experiment Data Handbook*, NASA TM X-58131, JSC-09166, National Aeronautics and Space Administration, Houston, Tex.
- Lognonné, P. (2005), Planetary seismology, *Annu. Rev. Earth Planet. Sci.*, *33*, 19.1–19.34.
- Lognonné, P., and C. L. Johnson (2007), Planetary Seismology, in *Treatise in Geophysics*, vol. 10, chap. 4, edited by G. Schubert, Elsevier, New York.
- Lognonné, P., J. Gagnepain-Beyneix, and H. Chenet (2003), A new seismic model of the Moon: Implications for structure, thermal evolution and formation of the Moon, *Earth Planet. Sci. Lett.*, *211*, 27–44.
- Mimoun, D., et al. (2012), Farside explorer: Unique science from a mission to the farside of the Moon, *Exp. Astron.*, *33*(2–3), 529–585, doi:10.1007/s10686-011-9252-3.
- Nakamura, Y. (1983), Seismic velocity structure of the lunar mantle, *J. Geophys. Res.*, *88*, 677–686, doi:10.1029/JB088iB01p00677.
- Nakamura, Y. (1992), Lunar—Catalog for lunar seismic data from Apollo Passive Seismic Experiment on 8-mm video cassette (EXABYTE) tapes, Univ. of Texas Institute for Geophysics, Austin.
- Nakamura, Y. (2003), New identification of deep moonquakes in the Apollo lunar seismic data, *Phys. Earth Planet. Inter.*, *139*, 197–205.
- Nakamura, Y. (2005), Farside deep moonquake and deep interior of the Moon, *J. Geophys. Res.*, *110*, E01001, doi:10.1029/2004JE002332.
- Nakamura, Y., J. Dorman, F. Duennbier, M. Ewing, D. Lammlein, and G. Latham (1974), High-frequency lunar teleseismic events, *Proc. Lunar Planet. Sci. Conf. 3rd*, pp. 2883–2890, Houston, Tex.
- Nakamura, Y., G. V. Latham, H. J. Dorman, and J. E. Harris (1981), Passive seismic experiment long-period event catalog, final version, Univ. of Tex. Institute for Geophysics Technical Report 18, Galveston, 1981 revised 2004.
- Nakamura, Y., G. V. Latham, and H. J. Dorman (1982), Apollo lunar seismic experiment—Final summary, *Proc. Lunar Planet. Conf. 13th*, pp. 117–123.
- Shiraishi, H., et al. (2010), Lunar BroadBand Seismometer System in the Japanese lunar landing mission SELENE-2: Its science goals and instrument details, AGU Fall Meeting, U51B-0039, San Francisco, Calif.
- Vinnik, L., H. Chenet, J. Gagnepain-Beyneix, and P. Lognonné (2001), First seismic receiver functions on the Moon, *Geophys. Res. Lett.*, *28*, 3031–3034, doi:10.1029/2001GL012859.
- Weber, R. C., P. Lin, E. J. Garnero, Q. Williams, and P. Lognonné (2011), Seismic detection of the lunar core, *Science*, *331*, 309–312.
- Wieczorek, M. A., et al. (2013), The crust of the Moon as seen by GRAIL, *Science*, *6120*, 671–675, doi:10.1126/science.1231530.
- Yamada, R., R. F. Garcia, P. Lognonné, N. Kobayashi, N. Takeuchi, T. Nébut, H. Shiraishi, M. Calvet, and J. Gagnepain-Beyneix (2013), On the possibility of lunar core phase detection using new seismometers for soft-landers in future lunar missions, *Planet. Space Sci.*, *81*, 18–31.